ELSEVIER

Catalysis Today 28 (1996) 193–203

CATALYSIS TODAY

Thermal stability and reactions of CH_2, CH_3 and C_2H_5 species on the metal surfaces

F. Solymosi

Institute of Solid State and Radiochemistry, A. József University and Reaction Kinetics Research Group, Hungarian Academy of Sciences, P.O. Box 168, H-6701 Szeged, Hungary

Abstract

The results obtained on thermal stability and reactions of C_xH_y hydrocarbon fragments on metal surfaces are discussed. C_xH_y species are produced by thermal and photo-induced dissociation of corresponding iodo compounds. Whereas CH_3 and CH_2 are mainly converted into CH_4 on Pt metals at 140–180 K, they recombine readily to yield C_2 compounds on Ag and Cu surfaces. The C_2H_5 reacted to form C_2H_4 and C_2H_6 on metal surfaces at 160–230 K. Effects of additives and coadsorbed species on the reactions of C_xH_y moieties are also examined.

Keywords: Thermal stability of hydrocarbon fragments; Metal surfaces

1. Introduction

Hydrocarbon moieties, C_xH_y, are important reaction intermediates in the catalytic synthesis of hydrocarbons and in the transformation of CH_4 into C_2H_6 both in the oxidative coupling on oxide surfaces [1–3] and under non-oxidative conditions on supported metals [4–10]. The study of their bonding and reactivity on catalysts is hampered by the fact that the catalytic reactions involving hydrocarbons occur at relatively high temperatures, where the lifetime of C_xH_y intermediates on the catalyst surface is very limited. One possibility for the production of a fragment C_xH_y at lower temperatures is the thermal dissociation of halogenated hydrocarbons. The characteristic features of the adsorption and dissociation of these compounds on metal surfaces have been discussed in a recent review [11]. The gas phase carbon–halogen bond energies in alkyl halides are as follow: C–I 55 kcal/mol, C–Br 70 kcal/mol, C–Cl 85 kcal/mol. In harmony with these data, the reactivity of alkyl halides with metals decreases in the order iodides > bromides > chlorides. As a result of this feature mostly iodide compounds are used to generate hydrocarbon fragments on solid surfaces.

In the present paper an account is given on chemistry of hydrocarbon fragments on metals, particularly on Pd(100) and Rh(111) surfaces; these two metals are being extensively studied in the laboratory of the author. Both metals were found to be active in the dehydrogenation of methane and in the reaction of CH_4–CO_2 to produce synthesis gas [7–9,12]. Emphasis will be given (i) on the production at hydrocarbon species of desired composition, (ii) on the thermal stability and reactions of these species on metal surfaces, and (iii) on the application of

SSDI 0920-5861(95)00242-1

the findings of surface science studies on the dehydrogenation of CH_4 on supported metal catalysts. Attention is also paid to the influence of different additives and coadsorbed species on the above processes.

2. Molecular orbital studies of adsorption of CH_3, CH_2 and CH moieties on Rh(111) surface

Before discussing the experimental results we briefly summarize the conclusions of a molecular orbital study of Koster and van Santen [24] on the bonding of CH_x fragments on Rh(111) surfaces.

The adsorption of hydrocarbon fragments was examined with the atom superposition and electron delocalization (ASED) and extended Hückel molecular orbital methods. Results were analyzed by calculating the local density of states (LDOS) and bond order overlap populations. It was found that CH is adsorbed on threefold sites, CH_2 on twofold sites and CH_3 on onefold sites in order to restore missing C–H bonds. The height of CH_x to the metal surface decreases with decreasing hydrogen content x, while the adsorption energy increases. CH_3 bonds on the Rh(111) mainly via σ type interactions of the n CH_3 orbital with surface metal atoms of the same symmetry. In case of the onefold adsorption, the highest occupied molecular orbital (n CH_3) has a large interaction with metal s, p_z and d_z^2 orbitals. For twofold adsorption it interacts mainly with the symmetric s, p_x, and d_{xz} metal group orbitals. Interactions of surface metal orbitals with the π and π^* orbitals are weak. As regards the coupling reaction of coadsorbed CH_2 and CH_3, a strong repulsion due to steric interaction of the hydro-

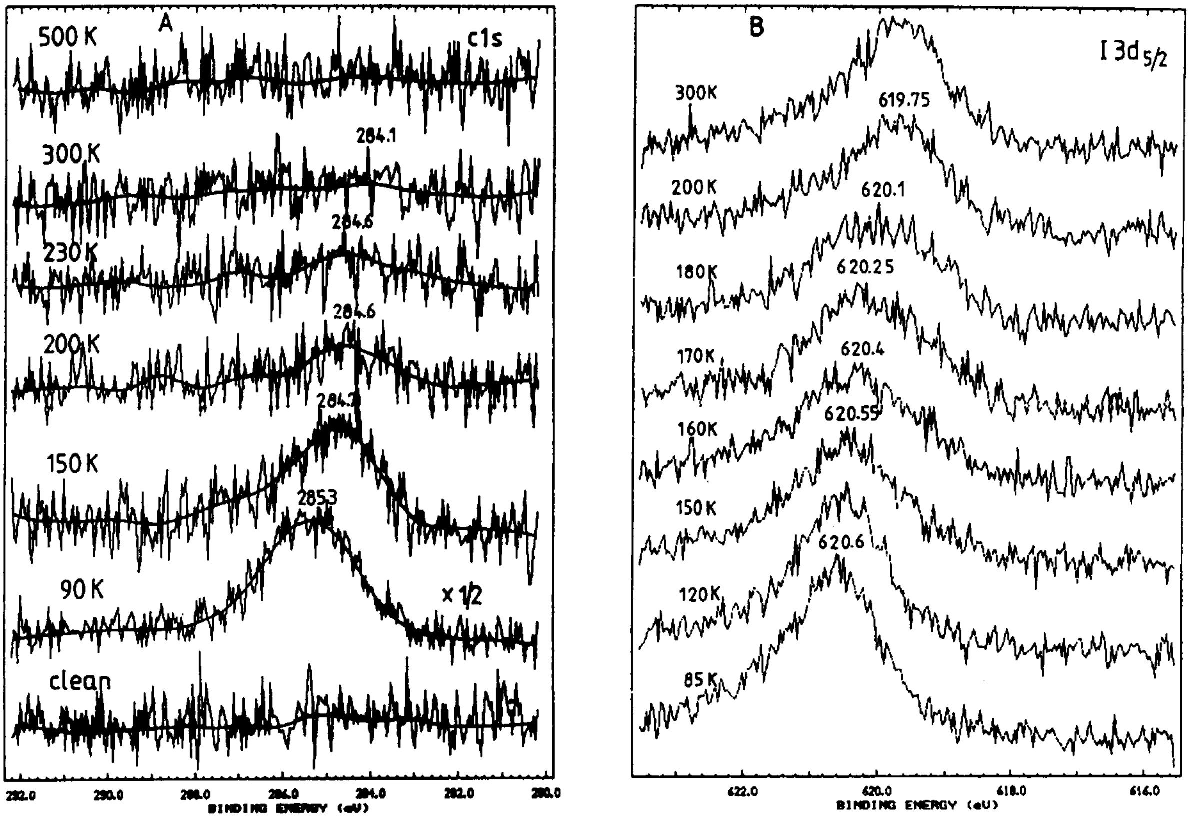

Fig. 1. XPS of C(1s) (A) and I($3d_{5/2}$) (B) of adsorbed CH_3I after heating the adsorbed layer to different temperatures.

gen atoms was found when the carbon–carbon distance was decreased. As a result the direct coupling reaction of CH_3 and CH_2 was not considered as a suitable reaction path for the C–C coupling reaction.

3. Formation and reactions of adsorbed CH_3

Methyl iodide adsorbs on metal surfaces with high sticking probability at 100 K, even up to multilayer coverages [11–15]. The adsorption is accompanied by a significant work function decrease (at monolayer $\Delta\phi = 1.1–1.6$ eV) indicating a dipole with the positive end pointed away from the surface. This is consistent with bonding of molecular CH_3I through the iodine atom, since alkyl halide molecules all have permanent dipoles with a positive methyl group. UPS spectra of molecularly adsorbed CH_3I suggest that the adsorption caused little distortion of the gas-phase molecular electronic structures. At high exposures multilayers form and desorb at 129–136 K [11–15].

As regards the dissociation of the molecule, it is a general observation that CH_3I adsorbs dissociatively at submonolayer coverage on most of the Pt metals even at 90–100 K yielding adsorbed CH_3 and I [11,15,19]. At higher coverages the adsorption is molecular: monolayer dissociates only at elevated temperatures (150–200 K), where the decomposition of CH_3 also proceeds. The dissociation can be easily followed by X-ray photoelectron spectroscopy (XPS) via the binding energy (BE) of I($3d_{5/2}$), as it differs by about 1.5–2.0 eV for molecularly adsorbed iodo compounds and for atomically adsorbed iodine. The ultraviolet photoelec-

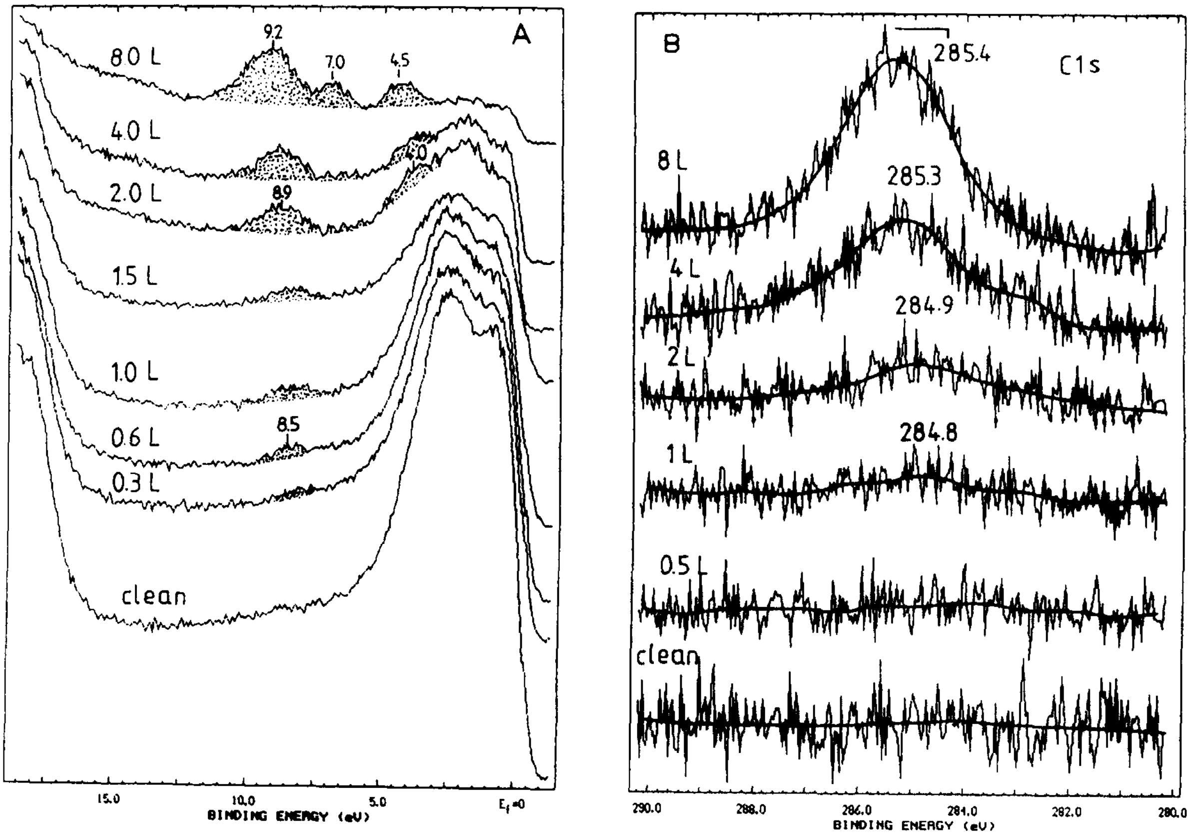

Fig. 2. (A) He(II) UPS and (B) XPS spectra for C(1s) signal as a function of CH_3I adsorption on Pd(100) at 85 K.

tron spectroscopy (UPS) can be also used, but this method is less sensitive than the XPS. High resolution electron energy loss spectroscopy (HREELS) is also applied in this area, as the characteristic vibrations of CH_3I and CH_3 are different. In this case the limited resolution of HREELS may cause a problem. Vibrational frequencies of adsorbed CH_3 on metal surfaces are listed in Table 1.

To illustrate the use of XPS method, XPS spectra of I($3d_{5/2}$) for adsorbed CH_3I on Pd(100) as a function of CH_3I exposure and annealing temperature are presented in Fig. 1 [15]. At low exposure a peak appeared at 619.9 eV, which gradually shifted to higher binding energy up to 620.7 eV with the increase of the exposure. When a monolayer is annealed, a clear shift occurred in the binding energy for I($3d_{5/2}$) from 620.6 to 619.7 eV in the temperature range of 160–190 K, indicating a change in its chemical state.

Table 1
Vibrational frequencies of (in cm^{-1}) adsorbed CH_3 group produced alkyl halide dissociation [a]

Vibr. modes	Pt(111)	Pt(111)	Cu(111)	Cu(111)	Rh(111)
$\nu a(CH_3)$	2925	2950	2950	2910	2920
$\nu s(CH_3)$	2775	2770	2820	2781	
$\delta a(CH_3)$	1425	1410	1370	1386	1350
$\delta s(CH_3)$	1165	1180	1180	1185	1185
$\rho s(CH_3)$	790	820		854	760
ν(M–C)	520	495			

[a] Data were taken from Ref. [19].

Characteristic UPS (He(II)) and XPS for C(1s) spectra as a function of CH_3I exposure on Pd(100) are depicted in Fig. 2. At low coverage, only one photoemission peak appeared in the He(II) spectra at 8.5 eV, which is due to 1e orbital of the pyramidal CH_3 radical formed in the dissociation of CH_3I. At high exposures, photoemission peaks developed at 4.5, 7.0 and 9.2 eV, which are characteristic of molecularly

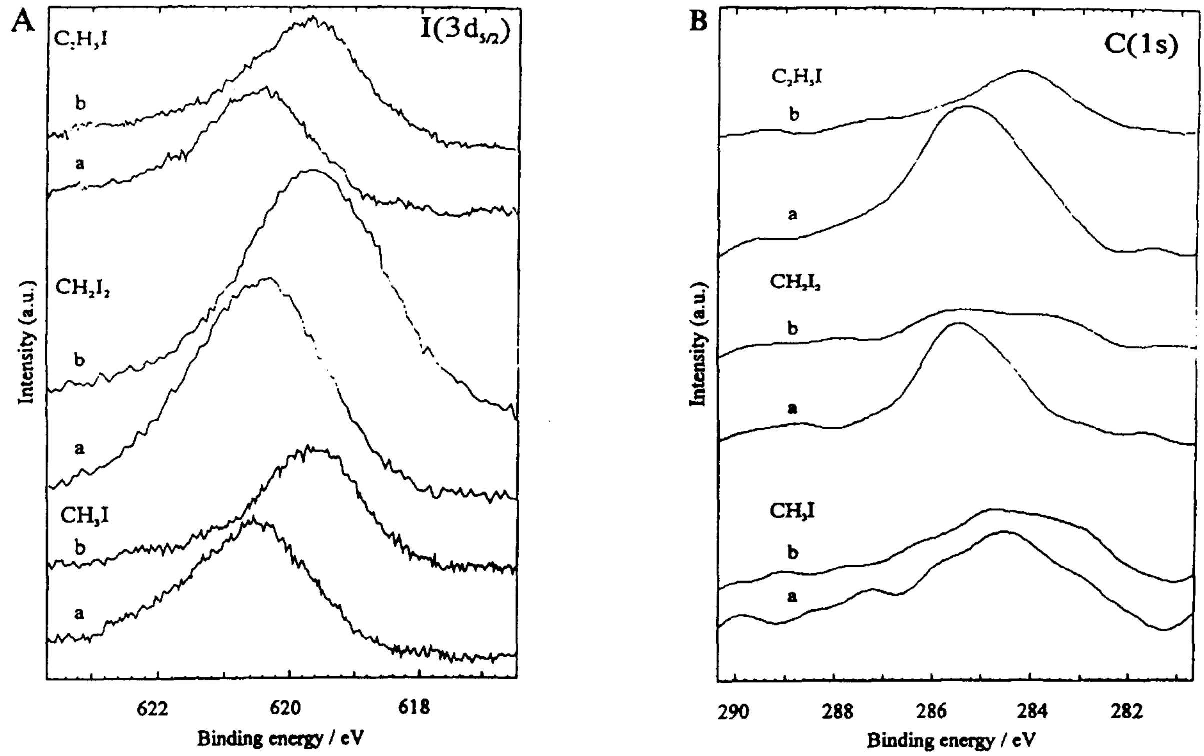

Fig. 3. XPS of I($3d_{5/2}$) (A) and C(1s) (B) of adsorbed CH_3I, CH_2I_2 and C_2H_5I (monolayer) before illumination (a) and after complete photo-induced dissociation (b).

Table 2
Selected binding energies C(1s) for adsorbed CH_x species on metal surfaces [a]

		Original compound	Binding energies (eV)
CH	Co	CH_2Cl_2	283.8
CH	Ni	CH_2Cl_2	283.8–284.0
CH_2	Co	CH_2Cl_2	284.9
CH_2	Ni	CH_2Cl_2	285.0–285.2
CH_2	Pd(100)	CH_2I_2	283.9
CH_2	Pd(100)	CH_2N_2	283.6
CH_3	Co	CH_3I	284.9
CH_3	Ni	CH_3I	285.6
CH_3	Ag(111)	CH_3I	284.6
CH_3	Pd(100)	CH_3I	284.6
CH_3	Pd(111)	CH_3OH	284.6
CH_3	Pd(111)	CH_3OH	284.7
CH_3	Pd(111)	CH_3OH	284.2
C_2H_5	Pd(100)	C_2H_5I	284.1

[a] Data were taken from Ref. [16].

adsorbed CH_3I. In the XPS, the C(1s) signal appeared at 248.8 eV at low exposure. The C(1s) peak shape and position remained constant up to 2.0 L exposure. This binding energy is very probably is associated with the same adsorbed species (CH_3) which gave a photoemission peak at 8.5 eV in the UPS. With further increase of the CH_3I exposure, the position of the C(1s) peak shifted to a higher binding energy, 285.3–285.4 eV, and became broader. This change in the C(1s) region is very likely the result of the formation of a multilayer. Selected binding energies for adsorbed CH_x species on metal surfaces are summarized in Table 2.

The complete dissociation of molecularly bonded CH_3I on Pd(100) can be also achieved at 90–100 K, when the adsorbed layer is irradiated with full arc of mercury lamp for an extended period of time [15]. This is demonstrated by XPS spectra presented in Fig. 3. The advantage of the photo-induced dissociation compared to thermal dissociation is the absence of secondary reactions of hydrocarbon fragments, which occur easily during the thermal processes at higher temperatures.

The reactivity of adsorbed CH_3 sensitively depends on the nature of the metals. On a Pd(100) surface the photoemission signal of CH_3 at 8.5 eV disappeared at 225–250 K [15]. The dominant mode of the reactions of CH_3 species is its decomposition to carbon and self-hydrogenation into CH_4

$$4CH_3 \rightarrow 3CH_4 + C$$

The peak temperature of methane formation was 160 and 170 K for Pt metals. Coupling of CH_3 on Pt metals occurred to a very limited extent (ethane was only 1–2% of that of methane formed).

The adsorbed CH_3 group exhibits a completely different behavior on Ag(111) surface [25]. Methane and hydrogen, the major products of the decomposition and self-hydrogenation of CH_3 species on Pt metals, are absent in the desorbing products. CH_3 groups recombine into ethane

$$2CH_{3(a)} \rightarrow C_2H_{6(a)}$$

which desorbs with $T_p = 257$ K. The ethane formation is a reaction limited process, as ethane adsorbs very weakly on the Ag(111) surface: no uptake of ethane was observed at 90–100 K.

Adsorbed CH_3 at high coverages behaves similarly on Cu surfaces where methyl coupling to form ethane is favored over dehydrogenation on both Cu(110) and Cu(111) surfaces [26–28]. The peak temperature of ethane desorption from Cu(110) varied between 400 and 450 K. However, at low coverages the primary products are methane and ethylene which are evolved simultaneously at 400–500 K. The differences between the two Cu surfaces are that on Cu(111) propylene is also formed and the CH_4/C_2H_4 ratio for Cu(110) is 2.1, whereas that for Cu(111) is 4.1.

4. Formation and reactions of adsorbed CH_2

Monolayer adsorption of CH_2I_2 on Pd(100) and Rh(111) resulted in a work function de-

Table 3
Vibrational frequencies (in cm^{-1}) of adsorbed CH_2 species [a,b]

Assignment	$CH_2(CH_2CO)$	$CH_2(CH_2N_2)$	$CH_2(CH_2CO)$	$CH_2(CH_2I_2)$
$\nu as(CH_2)$	2495	–	–	2940
$\nu s(CH_2)$	2870	2965	2970	
$\delta(CH_2)$	1295	–	1430	
$\omega(CH_2)$	1065	1165	1020	1190
$\gamma(CH_2)$	–	–	930	
$\rho(CH2)$	890	785	790	780
$\nu as(M-C)$	–	–	–	
$\nu s(M-C)$	–	–	650	650

[a] Data were taken from Ref. [20].

[b] The original compounds are in brackets.

crease of 0.75–0.85 eV [16,20]. The adsorption was dissociative at the submonolayer at 90–100 K and molecular at the monolayer. The dissociation of the compound can be completed by illumination, as indicated by the significant shift in the binding energy of $I(3d_{5/2})$ (Fig. 3). The

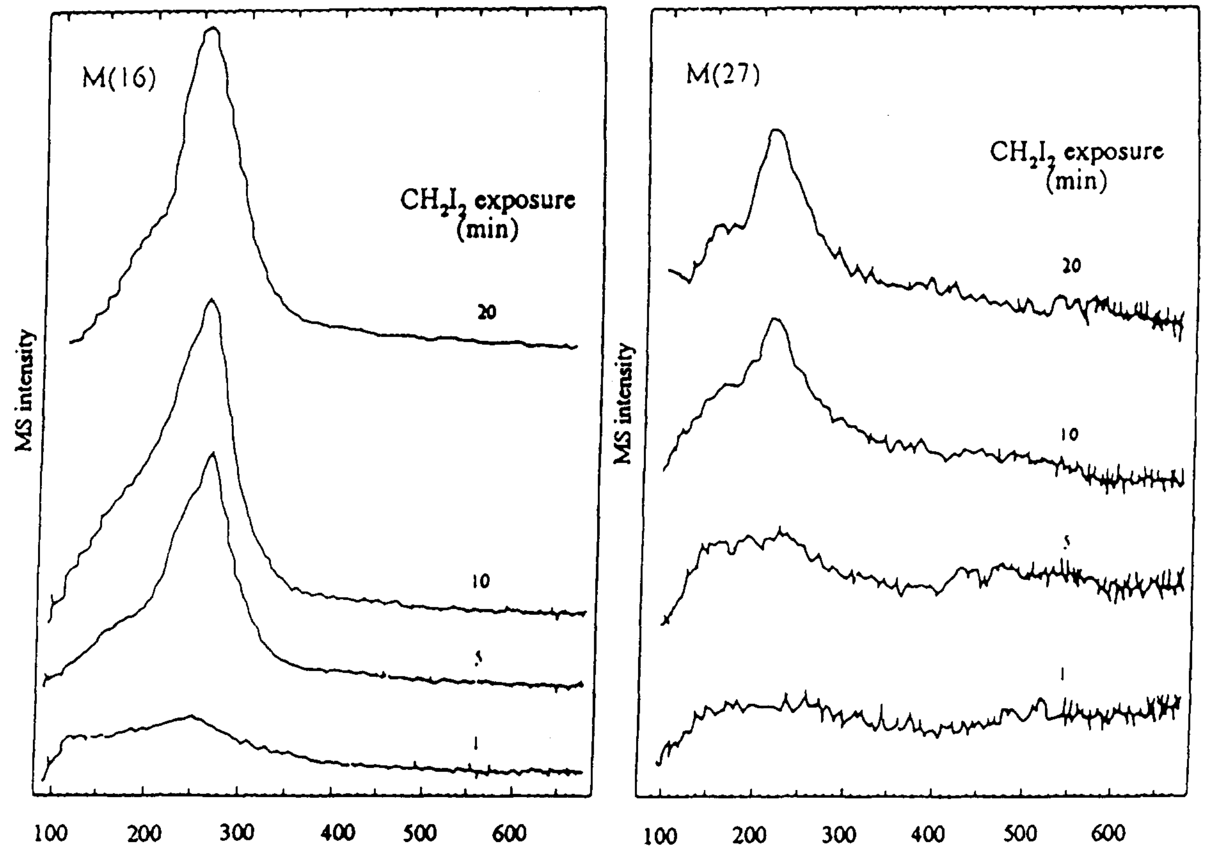

Fig. 4. TPD of CH_4 and C_2H_4 formed in the reaction of CH_2 on Rh(111) surface. CH_2 was generated by the dissociation of CH_2I_2 at 100 K.

primary products of the dissociation are CH_2 and I species. The photoemission signal of CH_2 species is located at 5.9–6.1 eV in UPS. Vibrational frequencies of adsorbed CH_2 are summarized in Table 3.

As regards the reactions of CH_2 on Pd(100) surface, the following features were established. A fraction of adsorbed CH_2 self-hydrogenates to give methane

$$4CH_2 \rightarrow 2CH_4 + 2C$$

which desorbs immediately after its formation at 150–300 K. On Pd(100) a significant fraction of CH_2 is dimerized to yield adsorbed ethylene, which desorbs in a broad peak between 140 and 250 K [16]. An increase in the surface concentration of CH_2 (by illumination of adsorbed CH_2I_2) markedly enhanced the formation of ethylene. In optimum case the ratio C_2H_4/CH_4 was 3.0–3.5 [17]. These features are in harmony with the theoretical calculation, which showed that the activation energy of coupling of the species CH_2 on metal surfaces is only 6–9 kcal/mol [29].

On the Rh(111) surface the dominant mode of the reactions of CH_2 was its transformation to methane [20]. Ethylene formation was very limited: the C_2H_4/CH_4 ratio varied between 0.01 and 0.03. Some TPD spectra for these product formations are displayed in Fig. 4. When the surface concentration of adsorbed CH_2 was increased by illumination of molecularly adsorbed CH_2I_2, the coupling reaction became more extensive: the C_2H_4/CH_4 ratio attained a value of 0.08–0.1. Interestingly, the characteristic losses of strongly adsorbed CH_2 on Rh(111) can be detected up to 350–400 K, when it decomposes to CH species. This high stability is very likely associated with the reduced tendency of CH_2 for coupling on Rh(111), in contrast to the Pd(100) surface. The limited formation of ethylene is in accordance with the recent calculation that the direct coupling of CH_2 on Rh(111) is not a suitable pathway for C–C formation due to the strong repulsion caused by the steric interaction of the H atoms [24].

As was expected, CH_2 species on the Cu(110) surface, generated by the thermal dissociation of CH_2I_2, recombined easily to give ethylene with a peak temperature of 290–300 K [27]. The reaction between adsorbed CH_2 and CH_3 to give C_2H_5 was also observed on the Cu(110) surface [27], which was not experienced for Pd(100) and Rh(111) surfaces.

5. Formation and reactions of C_2H_5

The adsorption of C_2H_5I on Pt metals is characterized by a work function decrease between 1.8 and 2.0 eV at the monolayer [17,21]. It is assumed that similarly to the other iodo-compounds, C_2H_5I bonds through the I atom. C_2H_5I adsorbs mostly molecularly even at submonolayer coverage. Its thermal dissociation occurs at 150–210 K, or following extended irradiation even at 90 K. This is illustrated by

Table 4
Vibrational frequencies (in cm^{-1}) of adsorbed C_2H_5 species [a,b]

	C_2H_5/Pt(111) (C_2H_5Cl)	C_2H_5/Cu(001) (C_2H_5Br)	C_2H_5/Si(111) $(C_2H_5)_2Zn$	C_2H_5/Rh(111) (C_2H_5I)	$C_2H<5$/Rh(111) $(C_2H_5)_2Zn$
ν(M–C)	484	370	630	385	510
$\rho(CH_3)$	941	855	900	850	860
ν(C–C)	1022	–	–	nr.	nr.
$\omega(CH_2)$	1173	1140	1230	1150	1140
$\delta(CH_3)$	1376–1430	1420	1430	1420	1430
ν(CH)	2918	2730,2900	2920	2910	2900

[a] The original compounds are in brackets.
[b] Data were taken form Ref. [21].

spectra displayed in Fig. 3. Photoemission lines for adsorbed C_2H_5 in UPS were registered at 6.4, 8.3 and 12.5 eV [17]. Vibrational frequencies of different modes of adsorbed C_2H_5 are listed in Table 4.

The ethyl moiety is a relatively stable species even on Pt metals. Characteristic TPD spectra for product formation on Pd(100) are shown in Fig. 5 [17]. Accordingly C_2H_5 dehydrogenates to yield C_2H_4 on one hand

$$C_2H_{5(a)} \rightarrow C_2H_{4(a)} + H$$

and hydrogenates to C_2H_6

$$C_2H_{5(a)} + H_{(a)} \rightarrow C_2H_{6(g)}$$

on the other hand. A fraction of the ethylene (π-bonded form) desorbs between 150 and 250 K, and another fraction (di-δ-form) is transformed into a vinyl species, which decomposes only above 450 K. The desorption of ethane is characterized with $T_p = 180$ K. As ethane does not adsorb on Pd(100) surface above 120 K, the release of ethane is a reaction limited process. The ratio of C_2H_4/C_2H_6 is 0.5. It is important to mention that no recombination of C_2H_5 to C_4H_{10} (butane) was observed. Similar features were established for the Rh(111) surface [21]. The main products of C_2H_5 reactions were again C_2H_4 and C_2H_6 with C_2H_4/C_6H_6 ratio of 0.3. Traces of butane ($T_p = 140$ K) were also detected. Besides ethylene and ethane, the formation of methane was also identified on the Pt(111) surface, which indicates the rupture of the C–C bond and the decomposition of hydrocarbon fragments formed [11,30].

On the Ag(111) surface C–H or C–C bond cleavage was not observed [31], and C_2H_5 was formed at the dissociation of C_2H_5I recombined into gas-phase butane around 190 K.

6. Effects of co-adsorbed species

Co-adsorbed species exerted significant influence on the reactivity of adsorbed alkyl and alkene species on metal surfaces. Site blocking, electronic effects and compound formation are considered for this phenomenon.

As CH_3 species was generated by the dissociation of CH_3I, the effect of co-adsorbed I on the chemistry of CH_3 was thoroughly explored.

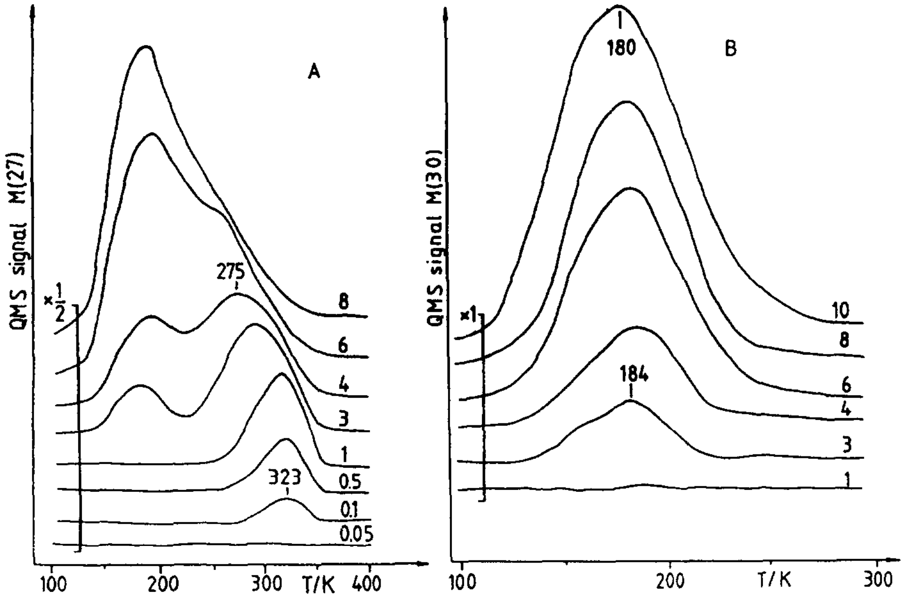

Fig. 5. TPD of C_2H_4 and C_2H_6 formed in the reaction of C_2H_5 on Pd(100) surface. C_2H_5 was generated by the dissociation of C_2H_5I at 90 K.

Although the binding energy of C(1s) in the XPS for adsorbed CH_3 is slightly shifted in the presence of co-adsorbed I, the chemical activity of CH_3 is not significantly altered.

A more pronounced effect was observed in the presence of co-adsorbed potassium on Pd(100) [13]. Potassium adatom promoted the rupture of the halogen–carbon bond, and at the same time, it increased the stability region of CH_3 from 250 to 350 K [13]. The stabilizing effect of K was explained by the formation of K–CH_3 surface compounds. This stabilization led to enhanced formation of ethane in the recombination of CH_3. In contrast, Bi atoms suppressed bond breaking reactions in CH_3I–Pt(111) systems [32], but greatly accelerated the reaction of

$$CH_3(a) + H(a) \rightarrow CH_4$$

The stability of CH_3 was also enhanced by co-adsorbed CO on Pd(111), Pd(100) and Rh(111) surfaces [21,33,34]. The self-hydrogenation of CH_3 to CH_4 occurred at temperatures which are up to 60–80 K higher than for the clean surface.

An occurrence of a chemical reaction was observed in the CH_3 + O/Rh(111) system yielding CO_2 and H_2O above 350 K [21,22]. It is assumed that the primary product of surface interaction is 'CH_3O' species. Attempts to identify the formation of this surface intermediate, however, brought no positive results, yet.

A more interesting reaction was recently explored for CH_2 species. CH_2 entered the reaction with co-adsorbed O atoms on Pt(111) [35], Pd(100) [34] and Rh(111) [23] surfaces resulting in the formation of a well measurable quantity of CH_2O. Some results obtained on Rh(111)

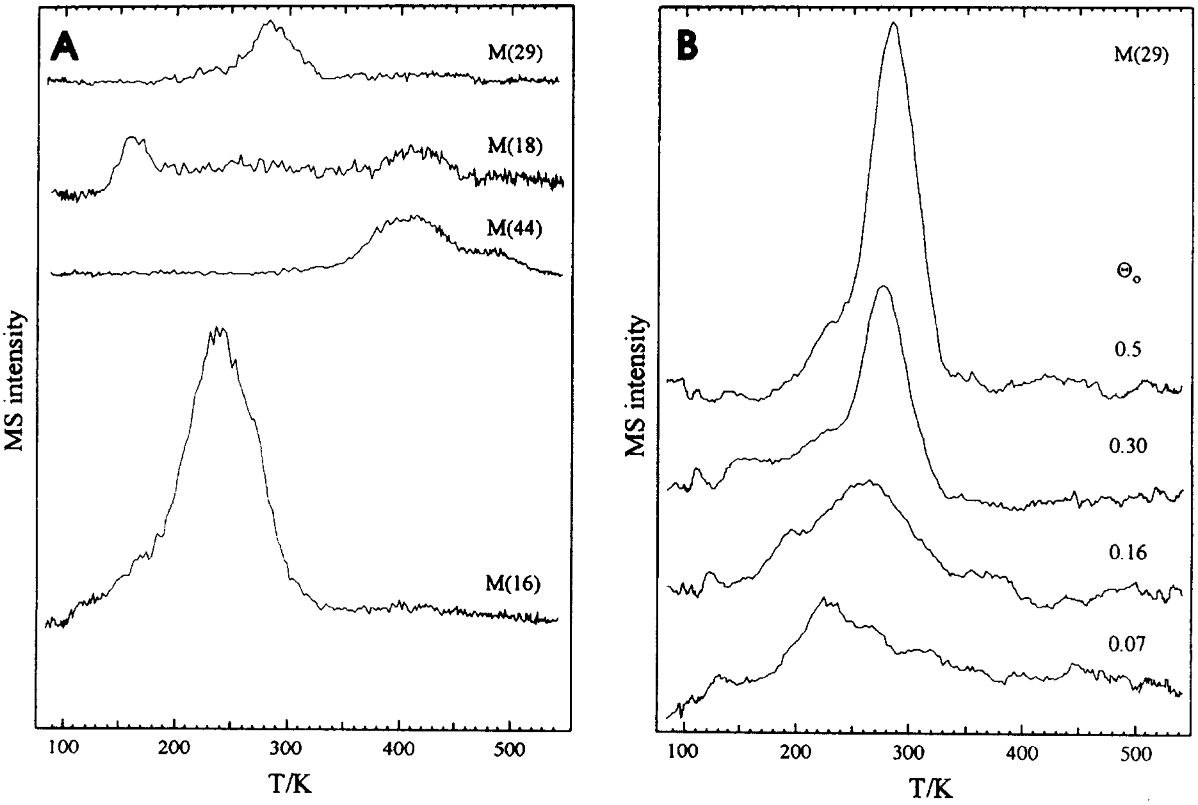

Fig. 6. (A) TPD spectra following the reaction of CH_2 with adsorbed O atoms on Rh(111) (Θ_O = 0.3) at 90 K. (B) Effects of oxygen coverage on the formation of CH_2O.

surfaces are plotted in Fig. 6. The production of formaldehyde started above 170 K and proceeded up to 300 K. Its formation was observed at the lowest O coverage, $\Theta_O = 0.07$, used. As the oxidation of CH_2 was not accompanied by any new spectral features in HREELS, it was concluded that CH_2O desorbs promptly after its formation. The total oxidation of adsorbed CH_2 occurred above 340 K yielding CO_2 and H_2O.

The reactivity of C_2H_5 species has been also influenced by co-adsorbed species [22]. Oxidation of C_2H_5 on Rh(111) surface started above 350 K. In addition to CO_2 and H_2O production, traces of C_2H_5OH ($T_p = 210$ K) and CH_3CHO ($T_p = 310$ K) were also detected by sensitive TPD measurements. The spectroscopic identification of these compounds by HREELS spectroscopy is in progress.

A dramatic influence on the reaction of C_2H_5 on both Pd(100) and Rh(111) surfaces was observed in the presence of Zn adatoms [18,36]. The C_2H_5 and Zn co-adsorbed system was produced by thermal and photodissociation of $(C_2H_5)_2Zn$. Whereas on I-covered Pd(100) surface no coupling reactions of C_2H_5 and its products were observed (Fig. 5); in the presence of Zn adatoms significant amounts of butene ($T_p = 183$ K) and butane ($T_p = 186$ K) were formed. At the highest surface concentration of C_2H_5 on Zn/Pd(100), the following ratios were measured: 1.0:4.6:6.3:8.5 for butane:ethane:ethylene:butene. On Rh(111) surface the coupling reaction was restricted only to C_2H_4 to yield C_4H_8.

7. Enhancement of ethane formation in the decomposition of CH_4 on Cu-Rh/SiO_2 catalyst

In a comparative study of the dehydrogenation of CH_4 on supported metals we found that Rh is one of the most effective metals [7,8]. An interaction between CH_4 and Rh/SiO_2 occurred even at 473 K to give H_2, C_2H_6 and surface carbon. At higher temperatures, 623–673 K, the initial conversion of CH_4 attained a value of 3.0–6.0%, which is, however, rapidly decayed to low values due to deposition of carbon. The amount of H_2 was more than 3 orders of magnitude higher than that of ethane. The conversion of methane sensitively depended on Rh loading and on the flow rate of methane. It was assumed that the primary step of the decomposition of CH_4 is the formation of CH_3 radical

$$CH_4 \rightarrow CH_3 + H$$

which recombines to give C_2H_6. The probability of this recombination is very limited mainly due to the fast decomposition of CH_3 at the temperature of CH_4 reaction as demonstrated by the results obtained on the CH_3/Rh(111) system. However, as both CH_3 and CH_2 species recombine readily on Cu surfaces [26–28], an attempt was made to enhance the ethane production in the CH_4 dehydrogenation by adding Cu to the Rh/Al_2O_3 catalyst. We found that the C_2H_6/H_2 ratio in the CH_4 decomposition at 573–673 K increased by a factor of 3–10 when Cu is added to the Rh/SiO_2 catalyst. As Cu is completely inactive towards CH_4 dissociation at 573–773 K, the possible reason of the higher C_2H_6/H_2 ratio is that CH_3 species formed on Rh may migrate on Cu where instead of decomposition they recombine to C_2H_6. Similar features have been observed for Ag + Rh/SiO_2 catalysts. Experiments to utilize these findings are in progress in our laboratory.

8. Conclusions

(1) Alkyl and alkene iodides were found to be suitable compounds to give hydrocarbon fragments of desired composition.

(2) The reaction pathways of hydrocarbon moieties on metal surface sensitively depend on their composition and on the nature of the metals. On Cu and Ag surfaces the dominant reaction route is the dimerization of hydrocarbon fragments. On Pt metals the situation is more

complex. CH_3 undergoes self-hydrogenation to yield methane. Its coupling to give ethane is very limited. The CH_2 species is also self-hydrogenated to methane, but at high concentration it readily dimerizes to ethylene. C_2H_5 reacted to form ethylene and ethane without methane formation. Recombination of C_2H_5 was not observed.

(3) Surface adatoms significantly influence the reactivity of hydrocarbon fragments; stabilizing effects and changes in reaction pathways were observed. This finding was exploited in the dehydrogenation of methane under non-oxidative conditions.

References

[1] D.M. Bibby, C.D. Chang, R.F. Howe and S. Yurchak, Methane Conversion, Studies on Surface Science and Catalysis, Vol. 36 Elsevier, Amsterdam, 1988.

[2] J.H. Lunsford, in L. Guczi, F. Solymosi and P. Tétényi (Eds.), Proc. of 10th Intern. Congress in Catalysis, Akadémiai Kiadó, Budapest, p. 103, 1993.

[3] Y. Ono, Catal. Rev. Sci. Eng., 34 (1992) 179.

[4] R.A. van Santen, A. de Koster and T. Koerts, Catal. Lett., 7 (1990) 1.

[5] T. Koerts, M.J.A.G. Deelen and R.A. van Santen, J. Catal., 138 (1992) 101.

[6] M. Belgued, P. Pareja, A. Amariglio and H. Amariglio, Nature, 352 (1991) 789; M. Belgued, H. Amariglio, P. Pareja, A. Amariglio and J. San-Just, J. Catal. Today, 13 (1992) 437.

[7] F. Solymosi, A. Erdöhelyi and J. Cserényi, Catal. Lett., 16 (1992) 399.

[8] A. Erdöhelyi, J. Cserényi and F. Solymosi, J. Catal., 141 (1993) 287.

[9] F. Solymosi, A. Erdöhelyi, J. Cserényi and A. Felvégi, J. Catal., 147 (1994) 272.

[10] F. Solymosi and J. Cserényi, Catal. Today, 21 (1994) 561.

[11] F. Zaera, J. Mol. Catal., 86 (1994) 221.

[12] A. Erdöhelyi, J. Cserényi, E. Papp and F. Solymosi, Appl. Catal. A, 108 (1994) 205.

[13] A. Berkó and F. Solymosi, J. Phys. Chem., 93 (1989) 12; F. Solymosi, A. Berkó and K. Révész, Surf. Sci., 240 (1990) 50; J. Kiss, A. Berkó, K. Révész and F. Solymosi, Surf. Sci., 240 (1990) 59.

[14] F. Solymosi, J. Kiss and K. Révész, J. Phys. Chem., 94 (1990) 2224; F. Solymosi, J. Kiss and K. Révész, J. Chem. Phys., 94 (1991) 8510.

[15] F. Solymosi and K. Révész, J. Am. Chem. Soc., 113 (1991) 9145; F. Solymosi and K. Révész, Surf. Sci., 280 (1992) 38.

[16] F. Solymosi and I. Kovács, Surf. Sci., 296 (1993) 171.

[17] I. Kovács and F. Solymosi, J. Phys. Chem., 97 (1993) 11056; F. Solymosi, I. Kovács and K. Révész, Catal. Lett., 27 (1994) 53.

[18] I. Kovács, N. Iost and F. Solymosi, J. Chem. Phys., 101 (1994) 4236.

[19] F. Solymosi and G. Klivényi, J. Electron Spectrosc. Relat. Phenom., 64/65 (1993) 499.

[20] G. Klivényi and F. Solymosi, Surf. Sci., 342 (1995) 168.

[21] L. Deák, A. Oszkó and F. Solymosi, Langmuir, in press.

[22] L. Deák and F. Solymosi, J. Catal., in press.

[23] F. Solymosi and G. Klivényi, J. Phys. Chem., 99 (1995) 8950.

[24] A.D.E. Koster and R.A. van Santen, J. Catal., 127 (1991) 141.

[25] X.L. Zhou, F. Solymosi, P.M. Blass, K.C. Cannon and J.M. White, Surf. Sci., 219 (1989) 294.

[26] J.-L. Liu and B.E. Bent, J. Vac. Soc. Technol. A, 10 (1992) 2202; C.-M. Chiang and B.E. Bent, Surf. Sci., 279 (1992) 79.

[27] J.-L. Liu and B.E. Bent, J. Phys. Chem., 96 (1992) 8529; C.M. Chiang, T.H. Wentzlaff and B.E. Bent, J. Phys. Chem. 96 (1992) 1836.

[28] J.-L. Lin, Ch.-M. Chiang, C.J. Jenks, M.X. Yang, T.H. Wentzlaff and B.E. Bent, J. Catal., 147 (1994) 250.

[29] E. Shustorovich and A.T. Bell, Surf. Sci., 205 (1988) 492.

[30] F. Zaera, Surf. Sci., 219 (1989) 453; F. Zaera, J. Phys. Chem., 94 (1990) 8350.

[31] X.-L. Zhou and J.M. White, Catal. Lett., 2 (1989) 375.

[32] M.B. Hugenschmidt, M.E. Domagala and C.T. Campbell, Surf. Sci., 275 (1992) 121.

[33] J.J. Chen and N. Winograd, Surf. Sci., 314 (1994) 188.

[34] I. Kovács and F. Solymosi, to be published.

[35] X.-L. Zhou, Z.-M. Liu, J. Kiss, D.W. Sloan and J.M. White, J. Am. Chem. Soc., 117 (1995) 3565.

[36] G. Klivényi, I. Kovács and F. Solymosi, to be published.